Materials and Design 193 (2020) 108862

Contents lists available at ScienceDirect

Materials and Design

journal homepage: www.elsevier.com/locate/matdes

Fire and mechanical properties of DGEBA-based epoxy resin cured with a cycloaliphatic hardener: Combined action of silica, melamine and DOPO-derivative

Aurelio Bifulco [a,b,1], Dambarudhar Parida [b,1], Khalifah A. Salmeia [b,c], Rashid Nazir [b], Sandro Lehner [b], Rolf Stämpfli [d], Hilber Markus [b], Giulio Malucelli [e,*], Francesco Branda [a,*], Sabyasachi Gaan [b,*]

[a] Department of Chemical Materials and Industrial Production Engineering (DICMaPI), University of Naples Federico II, Naples, Italy
[b] Laboratory for Advanced Fibers, Empa Swiss Federal Laboratories for Materials Science and Technology, Lerchenfeldstrasse 5, 9014 St. Gallen, Switzerland
[c] Department of Chemistry, Faculty of Science, Al-Balqa Applied University, 19117 Al-Salt, Jordan
[d] Laboratory for Biomimetic Membranes and Textiles, Empa Swiss Federal Laboratories for Materials Science and Technology, Lerchenfeldstrasse 5, 9014 St. Gallen, Switzerland
[e] Department of Applied Science and Technology, Politecnico di Torino, Viale Teresa Michel 5, Alessandria 15121, Turin, Italy

HIGHLIGHTS

- Self-extinguishing epoxy-silica nanocomposite at very low phosphorus loadings.
- In-situ sol-gel silica in the epoxy system prevented melt dripping.
- Intumescent system achieved significant reduction in heat release rate (~70%) and delay of the ignition time (~50%).

GRAPHICAL ABSTRACT

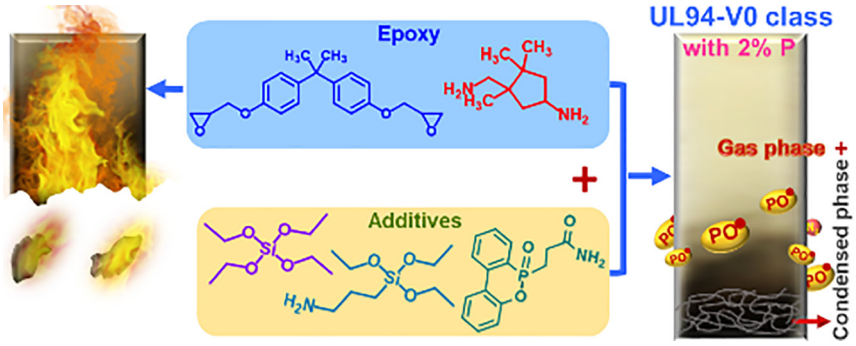

ARTICLE INFO

Article history:
Received 8 May 2020
Received in revised form 3 June 2020
Accepted 4 June 2020
Available online 6 June 2020

Keywords:
Epoxy-silica nanocomposite
Phosphorus flame retardant
In-situ sol-gel silica
Cycloaliphatic hardener
Fire

ABSTRACT

The effect of the addition of additives such as melamine (Mel), silica nanoparticles and a phosphorus-based compound, i.e. 3-(6-oxidodibenzo[c,e][1,2]oxaphosphinin-6-yl)propenamide (DA), on the fire and mechanical performance of a bisphenol A diglycidyl ether (DGEBA)-based epoxy resin cured with isophoronediamine has been investigated. A UL 94-V0 classification was achieved for epoxy resin containing DA at 2 wt% of phosphorus loading. However, addition of silica nano particles was necessary to avoid melt dripping. The incorporation of DA and Mel to the epoxy resin promoted a remarkable reduction (48% to 70%) in the heat release rate (HRR) values, a significant delay (up to 47%) in the ignition time in cone calorimetry experiments, and thus an increase (~75%) in the time to flashover. Evolved gas, thermal and fire analysis was used to propose the combined mode of action of DA, Mel and silica in the fire performance improvement of the epoxy system. Tensile and three-point bending flexural tests showed that the addition of DA increases the rigidity of the resin, resulting in a strong increase in the Young's modulus (up to 34%) and in a slight reduction in fracture strength, elongation break and toughness which is typical for non-reactive additives.
© 2020 The Authors. Published by Elsevier Ltd. This is an open access article under the CC BY-NC-ND license (http://creativecommons.org/licenses/by-nc-nd/4.0/).

* Corresponding authors.
E-mail addresses: giulio.malucelli@polito.it (G. Malucelli), branda@unina.it (F. Branda), sabyasachi.gaan@empa.ch (S. Gaan).
[1]Authors contributed equally.

https://doi.org/10.1016/j.matdes.2020.108862
0264-1275/© 2020 The Authors. Published by Elsevier Ltd. This is an open access article under the CC BY-NC-ND license (http://creativecommons.org/licenses/by-nc-nd/4.0/).

1. Introduction

Epoxy resins cured with various aliphatic amines are widely employed in the field of coatings, adhesives, casting, composites, etc. [1–5]. In addition to mechanical performance, stringent fire safety regulations must be fulfilled in these applications [6]. An improvement in the thermal stability and fire performance of epoxy systems can be achieved by using an aromatic hardener [7]. However, the adverse health effects of many aromatic amines have led to an increase in the use of aliphatic or cycloaliphatic amines as alternatives, even though this results in an overall decrease in the fire performance of the material [6]. Formation of corrosive/toxic combustion products in case of fire also prevents the use of halogen flame retardants [8]. Therefore, considerable effort has been made to develop flame retardants for epoxy systems with aliphatic hardener with low adverse health and environment effects.

The thermal stability and fire performance of epoxy resins can be improved through the inclusion of an inorganic additive (e.g., silica), which promotes the formation of a carbonaceous residue [9–12]. In this context, silica-epoxy hybrid nanocomposites via in-situ sol-gel method with low additive loading (<10 wt%) represent a very interesting method for the generation of materials with enhanced flame retardancy [13]. Such composites are characterized by the formation of very well-distributed silica domains in the matrix [13–15]. Hybrid silica-epoxy composites containing only 2.0 wt% inorganic additive can decrease the heat release rate by ~40% and prevents melt dripping [16], although such composites are not self-extinguishing.

Recently, epoxy resin has been cured with a curing agent obtained through the treatment of an environmentally benign phosphorous-based flame retardant DOPO (9,10-dihydro-9-oxa-10-phosphaphenanthrene-10-oxide) with desoxyanisoin. The material showed self-extinguishing capability, linked to a strong gas phase activity of DOPO and boosted char formation [17]. In general, the adoption of DOPO requires high loading (9.0 wt%) or the use of a phosphorous-based silane and modified hardener along with a nitrogen-based additive such as melamine as a synergist to achieve satisfactory flame retardancy [17,18]. Epoxy hybrid nanocomposites have been prepared using 4,4-diaminodiphenylmethane hardener and (3-aminopropyl)-triethoxysilane as coupling agent, along with DOPO and a nitrogen-based compound [19]. The phosphorus-nitrogen cooperative interaction resulted in a strong intumescence along with a gas phase flame inhibition of DOPO.

Currently, reactive approach in flame retardation has gained attention: the reactive P—H bond of DOPO allows covalent linkage to the epoxy network [20], resulting in an improved fire performance at lower phosphorus (P) loadings compared to the non-reactive approach. However, the use of an aromatic hardener was necessary in order to achieve satisfactory fire behavior. Recently, a DOPO derivative, namely 3-(6-oxidodibenzo[c,e][1,2]oxaphosphinin-6-yl)propanamide (DA) was synthesized using a green chemistry approach [21,22] and can be used as a nontoxic flame retardant for epoxy systems, where its gas phase activity may promote an efficient flame inhibition, as previously observed for polyester matrix [22]. Incorporation of this new flame retardant to in-situ silica-epoxy composites may help develop a material, which displays no dripping and improved flame retardancy, even though when a cycloaliphatic hardener is used as a component.

In this work a silica-epoxy nanocomposites were synthesized via "in-situ" sol–gel procedure from DGEBA and isophorone diamine as a cycloaliphatic hardener. To this resin system, DA and melamine were included alone or in combination to understand their role in flame retardancy and finally design a composite material with superior fire performance (UL 94-V0) with low P-loading (within 2.0 wt%). Nuclear Magnetic Resonance spectroscopy (NMR) and Differential Scanning Calorimetry (DSC) were used to investigate any possible reaction of DA with epoxy resin. The thermal and fire performance of prepared composites were studied in detail using Thermogravimetric Analysis (TGA), DSC, Cone Calorimetry, UL 94 vertical flame spread tests and other analytical techniques. In addition, the mechanical behavior of the silica-epoxy nanocomposites was also investigated.

2. Materials and methods

2.1. Materials

Tetraethyl orthosilicate (TEOS, >99%), (3-aminopropyl)-triethoxysilane (APTS, >98%), anhydrous ethanol, melamine, (>99%) and 1,8-diazabicyclo(5.4.0)undec-7-ene (DBU, ACS grade) were purchased from Sigma-Aldrich (Switzerland) and used as received. Bisphenol A resin (Epikote™ Resin 827) from Hexion Specialty Chemicals GmbH, Germany and isophorone diamine (IDA, Epikure™ Curing Agent 943) were used as received. DA (Fig. 1) was synthesized by a procedure as described in Section S1 of supporting information (SI) [22].

2.2. Preparation of in-situ silica-epoxy composites

The detailed composition and acronyms of composites are given in Tables 1 and S1. In a typical process [13,16], epoxy, DGEBA, and APTS with fixed weight ratio epoxy-APTS (Table 1) were stirred at 80 °C for 2 h followed by addition of TEOS, distilled water and ethanol mixture. Then the mixture was stirred vigorously for 90 min at 80 °C and subsequently the mixing vessel was opened for 30 min and the temperature was then raised to 100 °C. In silica containing composites TEOS/APTS weight ratio was maintained at 2. Then, DA was added to achieve 1.0 and 2.0 wt% P in the final composite followed by stirring for 60 min (Table 1). Some samples, were prepared with melamine as an additive. Finally, hardener (IDA) was added to the mixture at room temperature and mixed for 5 min. The resulting mixtures were degassed at reduced pressure prior to curing in a steel mold (40 °C/3 h) followed by post-curing (150 °C/2 h).

Unmodified-DOPO was also used as a reactive flame retardant additive for the epoxy, considering the reactivity of its P—H bond to epoxy group of the resin [20]. However, addition of unmodified-DOPO to the silanized DGEBA resin resulted in gelation of the resin, before the addition of hardener. Due to this fast gelation process, the epoxy resin-DOPO composite could not be prepared.

2.3. Characterization

NMR spectra were recorded using a Bruker AV-III 400 spectrometer (Bruker BioSpin AG, Switzerland). ^{1}H and ^{13}C chemical shifts (δ) were calibrated to residual solvent peaks. The ^{31}P chemical shifts were referenced to an external sample with neat H_3PO_4 at 0.0 ppm.

Phosphorus content in composites was determined by inductively coupled plasma optical emission spectrometry method (ICP-OES), on an Optima 3000 ICP-OES (PerkinElmer AG, Rotkreuz, Switzerland) instrument.

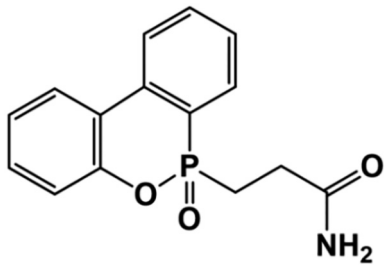

Fig. 1. Chemical structure of 3-(6-oxidodibenzo[c,e][1,2]oxaphosphinin-6-yl) propanamide (DA).

Table 1
Additives added to epoxy (107.75 g) and hardener (IDA, 26.8 g) to prepared FR-epoxy composites.

Entry	DA (g)	TEOS (g)	APTS (g)	Mel (g)	P (%)[a]	Sample code
1	–	–	–	–	–	EPO
2	27.4	–	–	–	1.64	DA1
3	41.1	–	–	–	2.58	DA2
4	–	–	–	13.7	–	Mel
5	41.1	–	–	13.7	2.39	DA2-Mel
6	–	6.92	3.61	–	–	Si2
7	41.1	6.92	3.61	–	2.27	Si-DA2
8	–	6.92	3.61	13.7	–	Si-Mel
9	27.4	6.92	3.61	9.13	1.58	Si-DA-Mel
10	41.1	6.92	3.61	13.7	2.23	Si-DA2-Mel

Individual additive loading % is given in Table S1. 0.85 g of ethanol and 2.75 g H_2O was used during preparation of composite containing Si (entry 6–10).
[a] P% was determined by ICP-OES.

ATR-FTIR spectra were recorded with a Bruker Tensor 27 FTIR spectrometer (Bruker Optics, Ettlingen, Germany), using a single reflection attenuated total reflectance (ATR) accessory with 4 cm^{-1} resolution, 32 scans and OPUS™ 7.2 software. In case of char, samples were collected from the burnt places and mixed properly prior to analysis.

The flammability of all composites was assessed by UL 94 VB vertical burning tests (IEC 60695-11-10, sample of 13 × 125 × 3 mm^3). An IR Camera (Type: Flir A40, FLIR Systems Inc., Wilsonville, USA) coupled with the UL 94 VB apparatus was used for recording the flame propagation. The IR video was recorded by ThermaCAM (Researcher Professional 2.10, FLIR Systems Inc., Wilsonville, USA) [23].

Thermogravimetric analysis (TGA) was performed on a NETZSCH TG 209 F1 instrument (NETZSCH-Gerätebau GmbH, Selb, Germany) under N_2 and air with a flow of 50 mL/min. Temperature range from 25 to 800 °C at a ramp of 10 °C/min was used for the analysis.

Differential scanning calorimetry (DSC) were performed on the DSC 214 Polyma instrument (NETZSCH-Gerätebau GmbH, Selb, Germany) at a heating rate of 10 °C/min (20 to 300 °C), under a N_2 flow (50 mL/min) by running two repeating cycles. The glass transition temperature (T_g) was determined by using the "tangent method" as the meeting point of tangents to the curve, traced on the baseline and the peak side, on the low-temperature peak side.

Cone calorimetry (Fire Testing Technology, East Grinstead, London, UK) was performed with an irradiative heat flux of 35 kW/m^2 (ISO 5660 standard) on a specimens (100 × 100 × 3 mm^3) placed horizontally without any grids. Parameters such as heat release rate (HRR), peak of heat release rate (pHRR), average specific extinction area (SEA), total smoke release (TSR), total heat release (THR) and the final residue were recorded.

Heat release rates (HRR) was determined using pyrolysis combustion flow calorimeter (PCFC) (Fire Testing Technology Instrument, London, UK) following ASTM D7309. ~7 mg of sample was exposed to a heating rate of 1.0 °C/s from 150 to 750 °C in the pyrolysis zone.

Pyrolysis-Gas Chromatography Mass Spectrometry (Py-GC–MS) were performed by taking about 30–100 μg of sample in a quartz tube (internal ϕ 1 mm × 25 mm) and loading it on the pyrolysis probe (Type 5200, CDS Analytical, Inc., Oxford, PA, USA). Samples were pyrolyzed at 800 °C under Helium for 30s. Volatiles were separated by a Hewlett-Packard 5890 Series II gas chromatograph and analyzed by a Hewlett-Packard 5989 mass spectrometer.

Direct inlet probe mass spectroscopy (DIP-MS) was performed in a Finnigan/Thermoquest GCQ ion trap mass spectrometer (Austin, TX, USA) equipped with a DIP module. ~1 mg of sample was placed in a quartz cup located at the tip of the probe and was inserted into the ionization chamber operating at ionization voltage of 70 eV, temperature of the ionic source of 200 °C and pressure <10^{-6} mbar. A probe temperature was run from 30 to 450 °C at 50 °C/min.

Energy dispersive X-ray spectroscopy (EDX) was carried out using an Inca X-sight device from Oxford Instruments (Tokyo, Japan) mounted on a S-4800 SEM from Hitachi (Tokyo, Japan). EDX spectra were recorded at voltage of 20 kV and emission current of 15 mA.

Tensile tests and **Three-point bending** test were performed on a Zwick/Roell Z100 (Zwick/Roell, Ulm, Germany) tester. Tensile tests were determined using 9 dumbbell-shaped specimens (ASTM D638-Type I, standard dimensions) with a crosshead speed of 5 mm/min. **Three-point bending** tests was performed as per ASTM D790 standard, using 5 kN load cell and 45 cm distance between the two supports.

3. Results and discussion

3.1. Chemical characterization of the in-situ silica-epoxy composites

Disappearance of characteristic ATR-FTIR absorption bands of the uncured epoxy resin **EPO_WH** (Fig. S1) at 970 cm^{-1}, 912 cm^{-1} and 870 cm^{-1} after curing in **EPO**, in-situ silica-epoxy (**Si2**) and in-situ silica-epoxy system with melamine and DA (**Si-DA2-Mel**) confirmed the completion of reaction. Appearance of bands between 1050 cm^{-1} and 1150 cm^{-1} in **Si2** indicated the formation of silica domains of ~1.25 nm size through the sol-gel reactions under similar condition reported in literature [16]. Detailed ATR-FTIR analysis in Section S2 of SI are consistent with the chemical composition of composites.

To study any possible reaction between amide group of DA (Fig. 1) and the oxirane rings of the epoxy resin, mixture of DA and epoxy resin was processed to simulate the curing process (Section 2.2) and resulting product was analyzed by ^{13}C NMR, ^{1}H NMR, and ^{31}P NMR (DMSO-d_6). A simulation of a base catalyzed reaction of DA with the epoxy resin was also attempted, by adding DBU as a catalyst DA-epoxy resin mixture prior to curing (**Uncured_EPODA**, Table S2). For both experiments, mixtures were prepared keeping epoxy/DA weight ratio 2.6 as used for **DA2** (Tables 1, S1). All peaks in ^{13}C NMR spectra (Fig. S2) of both samples can be assigned to DGEBA [24]; particularly those of oxirane group (44.2 ppm (C1), 50.2 ppm (C2)). Peaks for C-atoms linked to -OH that would form in the case of reaction with DA were not detected. Similarly, all signals in ^{1}H NMR spectra of sample

containing DBU can be assigned to the unreacted epoxy resin (details in Fig. S3). ^{31}P NMR spectrum of sample containing DBU shows the peaks of the unreacted DA (37.2 ppm, Fig. S4) [22,25]. NMR analysis confirmed the absence of reaction between DA with epoxy resin and DA can be considered as a non-reactive additive in current matrix. Absence of any exothermic peak in the DSC thermogram of epoxy resin-DA mixture (epoxy/DA = 2.6, weight ratio) with 5 wt% DBU on the weight of DA (i.e. **Uncured_EPODA**) (Fig. S5, Table S2) confirmed the lack of reaction between DA and epoxy resin. Endothermic peak at ~170 °C corresponding to the melting point of DA also confirmed the absence of reaction for DA with epoxy resin [22,25].

3.2. Thermal analysis

Absence of any exothermic peak in the first heating cycle of DSC analysis confirmed the completeness of the curing. The glass transition temperature was determined by using the "tangent method" by following the procedure reported in Section 2.3. A significant reduction in the T_g of composites containing silica alone or in combination with DA and melamine (Fig. 2) highlights the negative influence of hybrid co-continuous network of silica on epoxy chains mobility [16]. Further reduction in T_g of samples containing DA (Fig. 2) can be due to a plasticization effect of non-polar groups of DA (aromatic and alkyl chains) by breaking the inter-chain interactions [26], while, the amide group of DA interacts with the epoxy group of DGEBA to assure compatibility.

Figs. 3 and S6 show the TGA curves and the thermal behavior of epoxy resin cured with IDA can be interpreted on the basis of the mechanism reported in the literature [27,28]. In N_2 atmosphere composites decompose through a main step around 350 °C (Fig. 3). These results are in agreement with the degradation of an aliphatic epoxy resins [28–30]. Appearance of a third degradation step below 300 °C (in air) in melamine containing samples, can be attributed to the decomposition of melamine to ammonia and subsequently to N_2 in presence of O_2 [31]. Earlier mass loss in DA containing samples (Figs. 3a,c and S6a, c) can be attributed to: (i) the formation of acidic phosphorus species via degradation of DA, (ii) the acidic characteristics of in-situ sol-gel silica [16] and (iii) the production of non-flammable volatiles (phosphorous species and N_2) [32,33]. In air, the ratio of the mass loss in the first step (< 400 °C) and second step (400–600 °C) decreased in presence of DA and melamine, suggests the improved thermo-oxidative stability of composites and formation of aromatic char at high temperatures [22].

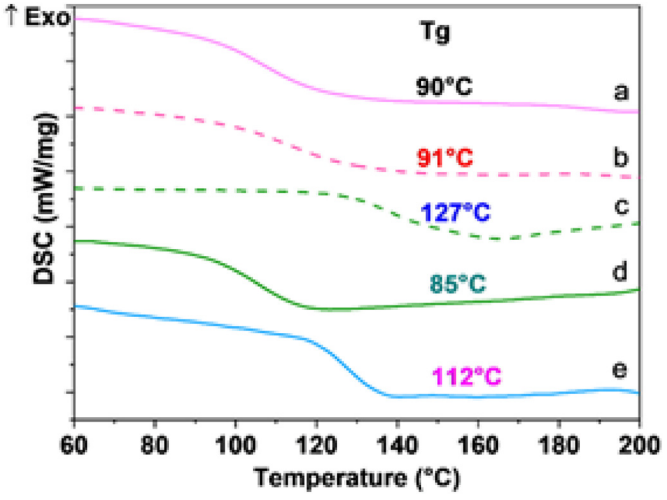

Fig. 2. DSC thermograms (second heating cycle) of (a) **Si-DA-Mel**, (b) **Si-DA2-Mel**, (c) **EPO**, (d) **DA2** and (e) **Si2**.

The increase in the residues DA-containing nanocomposites during TGA in air (Table S3) supports the argument of stable char formation [25,34,35]. The combination of DA and silica nanoparticles significantly improves the thermo-oxidative stability of **Si-DA2** (9.0% residue) compared to **EPO** (0.7% residue) at 800 °C (Table S3). This can be attributed to acidic characteristics of the in-situ sol-gel silica and the formation of acidic phosphorus species, hence promoting the carbonization process via dehydration of epoxy resin [16,22]. Additionally, degradation of silica-epoxy networks during combustion of **Si-DA2** leads to formation of silica substructures [16] and condensation of the silanol groups of Si-O-Si network with the decomposition products of DA (i.e. polyphosphoric acid) form a stable ceramic thermal shield on the char [22,35,36]. This thermal shield works as a barrier and prevents the diffusion of decomposed gas and oxygen from air into the material. In case of **Si-DA-Mel** and **Si-DA2-Mel**, release of N_2 and other volatiles during decomposition of melamine disrupts the progressive formation ceramic shield, resulting slightly lower residue during TGA in air [16,33,35].

3.3. Fire behavior of the in-situ generated silica-epoxy materials

Epoxy composites were subjected to vertical flame spread test to assess their flammability. Interestingly, **EPO**, **DA1**, **Si2**, **Si-Mel** and **Mel** results were not classifiable (Table S4), though a coherent char was observed in silica containing composites (Fig. S7b). Additionally, presence of silica in the epoxy matrix prevented dripping (Table S4), due to increase in the melt viscosity of the burning system [16]. The addition of DA to the epoxy resin is crucial to obtain UL 94-V0 classification and samples containing DA (2.0 wt% P) burns partially, producing a very coherent char (Fig. S7c). This suggests a strong flame inhibition action of DA from the early stage. A decrease in flame inhibition observed on subsequent application of flame at the same place is due to the lower concentration of the DA in the already burned area (**DA2** and **DA2-Mel** in Table S4). Afterflame times (t_1 and t_2, in Table S4) of these two samples reveals that, decomposition of melamine in **DA2-Mel** during burning produces nitrogen-based volatiles which leads to the dilution of flammable volatiles and decreasing the t_2 extinguishing time. Samples containing only 1.0 wt% of P did not achieve any classification in the UL 94 VB test without the addition of melamine and silica precursors.

Fig. 4 shows the burning behavior of composites recorded by an IR-camera during UL 94 vertical burning test. In particular, the burning process of **EPO** and **Si2** can be divided into three main steps: (I) *Contact phase:* material captures the flame followed by rapid increase in surface temperature. (II) *Middle flame phase*: the front flame moves and consumes the material; temperature increases further with production of volatiles, which feed the flame in the gas phase. (III) *End flame phase*: the flame reached the holding clamp and envelops the sample. In agreement with UL 94 standards, the flame was applied to **EPO** and **Si2** samples for 10 s and IR images were captured after removal of the flame (contact phase), when the flame reached the middle of the sample (middle flame phase) and when the flame reached the holding clamp and enveloped the sample (end flame phase). In the case of **Si-DA2-Mel**, as it shows self-extinguishing capability, the temperatures and IR images were taken at the end of the flame application (contact phase), when the surface temperature started rising quickly along the system after ~10 s (middle flame phase) and immediately following the second flame application according to UL 94 standard (end flame phase).

The addition of 2.0 wt% silica (**Si2**) lowers the middle and last phase temperatures compared to in **EPO** (Fig. 4a, b). On the other hand, flame propagation in case of **Si-DA2-Mel** was very limited and rapidly stopped once the flame was removed. Therefore, as previously described, a second flame was applied for 10 more seconds as per UL 94 standards (Fig. 4a, b) and significant reduction in middle and last phase temperature with self-extinguishing behavior was observed. In **Si-DA2-Mel**. The endothermic decomposition of DA [22,25] and melamine [32–34] in a combination with an increased thermo-oxidative stability due to DA

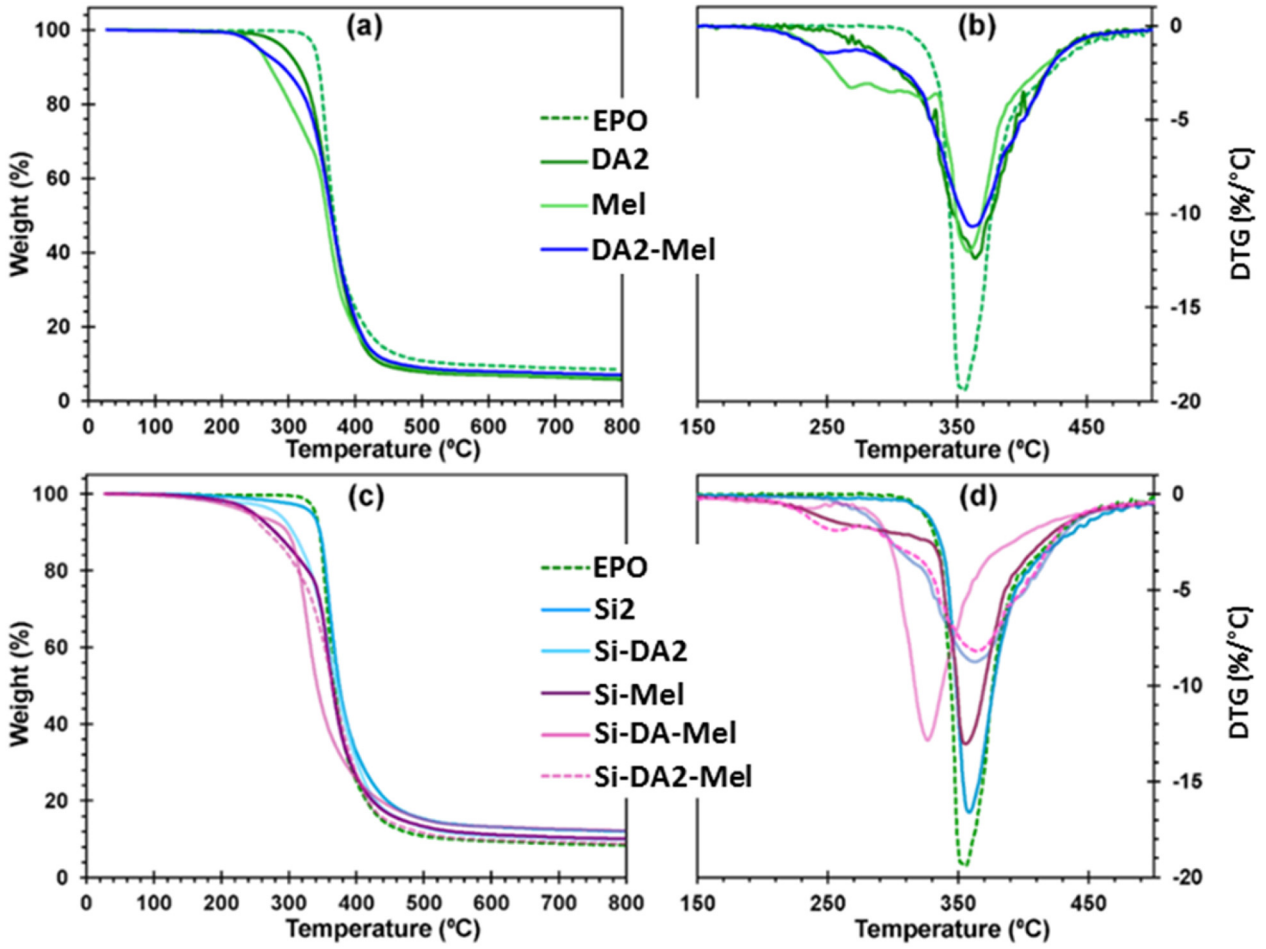

Fig. 3. (a, c) TGA curves and (b, d) DTG curves of **EPO** and epoxy composites under N_2.

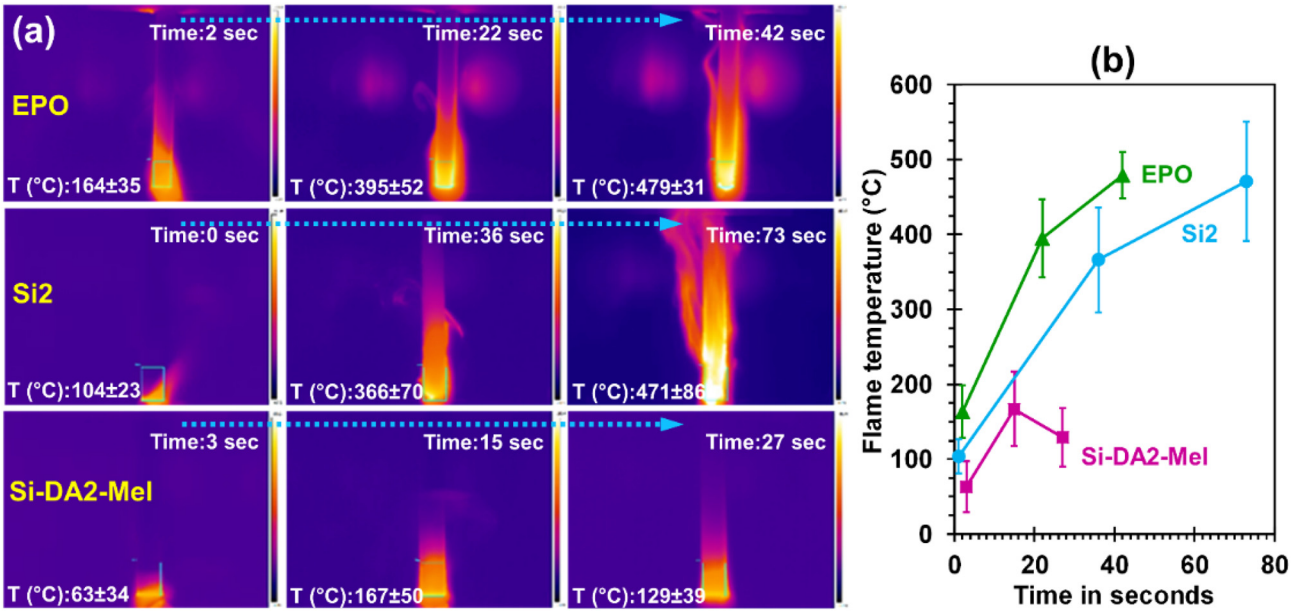

Fig. 4. (a) IR camera images showing flame profiles and temperatures at "contact", "middle" and "end" phases for **EPO**, **Si2** and **Si-DA2-Mel** during UL 94 vertical burning test. (b) Change in flame temperature with time measured by IR camera during UL 94 vertical flame test and decreasing flame temperature after 15 s in case of **Si-DA2-Mel**, shows its self-extinguishing behavior. For **EPO** and **Si2** the IR camera images and temperature at each phase were taken by following the procedure described in Section 3.3. Whereas, due to its self-extinguishing nature of **Si-DA2-Mel**, the IR camera image and temperature were recorded immediately after second flame application (10 more seconds), i.e. end phase stage.

and silica achieved ~60% lower temperature during the middle flame phase compared to **EPO** and **Si2** (Fig. 4b).

PCFC separately reproduces the condensed phase and gas phase processes of flaming combustion in a non-flaming test by controlled pyrolysis of the sample in an inert gas stream followed by high temperature oxidation of the volatile pyrolysis products. Therefore, the PCFC can be considered a very suitable instrument to study the gas phase activity of flame retarded systems as compared with cone calorimeter, where the combustion occurs as a continuous process in air condition. PCFC analysis indicated a strong influence of DA in reducing the HRC (i.e. the maximum rate of heat release divided by the heating rate in the PCFC test is a derived property called the "heat release capacity" which is related to flame resistance and fire performance) of epoxy resin by 56% (Fig. 5a and Table S5). However, limited residue, highlights gas phase activity of DA [22]. A narrow HRR curves of **EPO**, **Si2**, **Mel** and **Si-Mel** (Fig. 5a) indicates a large amount of heat released in a short time. Conversely, broad and flattened HRR curves of DA containing composites indicates flame inhibition of DA from the beginning via suppression of active oxygen radicals and resulting in a slow heat release over a longer period of time [22,34,36]. As a result, DA in the epoxy resin with only 2% of P-content achieved UL 94-V0 classification. However, for sample with P-content lower than 2% (**Si-DA-Mel**) displayed a sharper and higher intensity heat release peak compared to **Si-DA2-Mel** (Fig. 5a). The addition of melamine alone or in combination with DA to **EPO** led to an increase in the HRC (Table S5), this can be attributed to the exothermic oxidation of ammonia [31,32].

During cone calorimetry, reduction of HRR (ranging from 48% to 70%), THR and MLR (Mass Loss Rate) are more pronounced in case of composites containing DA with or without melamine (Fig. 5b, Table S6), though the presence of silica alone significantly decreases aforementioned parameters. The strong increase in CO/CO_2 ratio (Table S7) agrees with the hypothesis that DA acts dominantly in the gas phase and the formation of phosphorus species in gas phase lead to an incomplete combustion and formation of CO. These phosphorous species interrupt and slow down the branching and chain reactions of the hydrocarbon oxidations in the gas phase, thus reducing the heat production, known as flame inhibition [22,34]. In agreement with the PCFC measurements, broadening of HRR curve was observed in presence of DA (Fig. 5b). Degradation of melamine to N_2 dilutes the combustible gases [31,32] and delays the time of peak heat release and eventually time to ignition (**DA2-Mel**, **Si-DA2-Mel**, Fig. 5b and Table S6). The increase in residue at the end of the cone calorimetry tests (**Si-DA2**, Table S6) confirmed the condensed phase action of DA along with silica nanoparticles (Section 3.2). An increase in the residue was also observed in composites containing silica, DA and melamine (Fig. S8). Incorporating all these additives in the composite (**Si-DA2-Mel**), intumescence and a delay in the ignition time (~47%) was observed (Fig. S8d, Table S6). This can be ascribed to dehydration of the matrix by acidic silica and phosphorous species formed during combustion as a result a swollen carbonaceous char was formed (Fig. S9) [33,36].

Dimensionless measure known as Flame Retardancy Index (FRI) was calculated for comparison with other polymeric composites (Section S7, Table S6) [37,38]. Sample **Si2** exhibited low FRI value of (1.7) and thus was classified as "poor". Due to strong gas phase activity of DA sample **DA2** achieved highest FRI of 7.9 and was classified as "good" despite low TTI (time to ignition) value, which can be detrimental in real fire situation. Combination of silica and DA (**Si-DA2**) resulted a slight improvement in FRI (3.4) compared to **Si2**. Whereas, adding DA and melamine together (**DA2-Mel**) achieved a classification "good" with FRI of 6.6, predominantly increasing the TTI significantly. Combining all three additives to the epoxy resin (**Si-DA2-Mel**) achieved FRI of 7.5 with highest TTI of 56 ± 4 s (Table S6).

To further understand the role of melamine, time to flashover (TTF) and flame propagation index (FPI) were calculated (Sec. Table S6) [36,39]. FPI depends on the flammability (i.e. front flame movement, Fig. 4) and the TTF is the time available to escape a fire in a confined space [39]. It is worth mentioning here that, composites with melamine (**DA2-Mel** and **Si-DA2-Mel**) showed highest TTF (4 min) with slow flame propagation rate, characterized by low FPI (Table S6). The addition of DA results an overall increase in total smoke release (TSR, Table S7). An increase in the SEA (Smoke Extension Area), CO and CO_2 yields was also observed which is common for FR materials with gas phase activity [40].

3.4. Thermal decomposition and flame retardant mechanism studies

To further understand the decomposition mechanism and the influence of the various additives on the evolved gases, PY-GC–MS and DIP-MS were performed on **EPO**, **Si2** and **Si-DA2-Mel**. The most abundant products were recognized as bisphenol A, 4,4′-(cyclopropane-1,1-diyl) diphenol, 4-isopropylphenol, 4-isopropenylphenol, phenol, benzene, naphthalene, toluene, 2-methylpent-2-en-1-ol, 3-hydroxy-2-methylpentanal, o-cresol, 2-ethylphenol, and 2-allyl-4-methylphenol along with low amounts of aromatic products, as already reported for similar systems [27,29,30]. The presence of dibenzofuran, a decomposition product of DOPO, was also observed for **Si-DA2-Mel** [22,41].

DIP–MS analysis also confirmed the presence of the above-mentioned decomposition products (Fig. 6). Unlike in **EPO**, composites containing DA and melamine starts to decompose at very early stage (~200 °C) and a large amount of species were released at 350 °C for **Si-DA2-Mel**, which is in agreement with TGA results in N_2 (Fig. 3a and c). Analyzing the DIP-MS data of **Si-DA2-Mel** from 200 to 350 °C revealed the formation of major decomposition products which are summarized in Table S8 with respective thermograms presented in Fig. S10. The presence of these species was also observed for DA in polyester

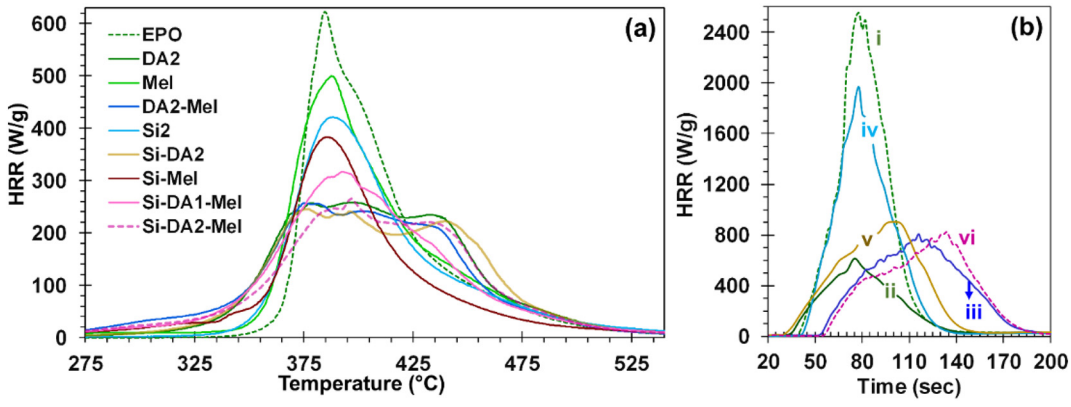

Fig. 5. (a) Heat release rate (HRR) of samples measured using PCFC. (b) HRR of (i) **EPO**, (ii) **DA2**, (iii) **DA2-Mel**, (iv) **Si2**, (v) **Si-DA2** and (vi) **Si-DA2-Mel** measured by cone calorimeter.

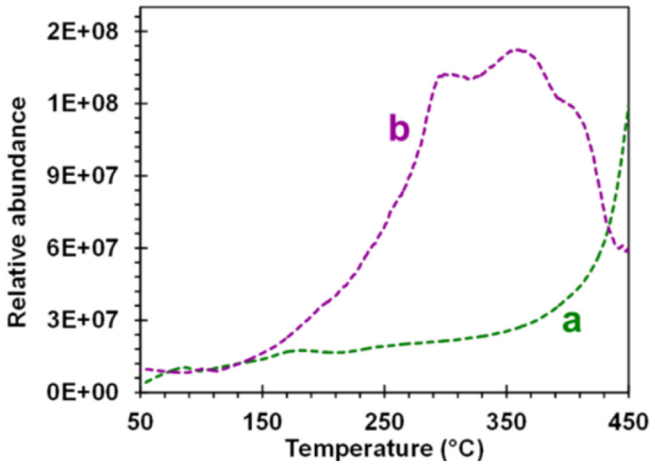

Fig. 6. DIP-MS total ion thermograms of (a) **EPO** and (b) **Si-DA2-Mel**.

matrices [22,41]. According to the DIP-MS results (Table S8 and Scheme 1), phosphorus species were released once the P—C bond of DA breaks [22,41]. Previous reports suggest that the decomposition pathway for epoxy resins in an inert atmosphere and at high temperature begins with the elimination of water from the secondary alcohol group [29,30]. Subsequently, the resulting allylic bonds, aromatic and ether linkages undergo homolytic cleavages and H-transfer reactions, leading to the formation of radicals and yield bisphenol A, 4,4′-(cyclopropane-1,1-diyl)diphenol, 4-isopropylphenol, 4-isopropenylphenol, phenol as decomposition products. Analysis of DIP-MS data for **EPO** and **Si-DA2-Mel** (Fig. S11, Table S9), proved the formation of the major decomposition products of pristine epoxy as bisphenol A, 4,4′-(cyclopropane-1,1-diyl)diphenol, 4-isopropylphenol, 4-isopropenylphenol and phenol. The same species were also detected using PY-GC–MS. Therefore, the collected experimental results are in good agreement with previous reports [29,30].

Fig. S11 shows the relative abundance bisphenol A, 4,4′-(cyclopropane-1,1-diyl)diphenol, 4-isopropylphenol, 4-isopropenylphenol and phenol released from **EPO** and **Si-DA2-Mel**. The decomposition of the DA produces a large amount of phosphorous species from 200 to 400 °C, where the epoxy resin shows low relative abundance of its main volatile compounds (Figs. 6 and S11). DIP-MS analysis of **Si-DA2-Mel** showed the formation of major fragments like DOPO radical (*m/z* 215) and benzofuran (*m/z* 168). Benzofuran in the gas phase is an indirect proof for the decomposition pathway of DOPO radical producing PO• (*m/z* 47) (Table S8) [25,41]. The strong gas phase activity of the DA suggested by the PCFC results may be related to the PO• produced during the pyrolysis. In air PO• can act in the gas phase and consume active H• and OH• species in a flame by recombining with them

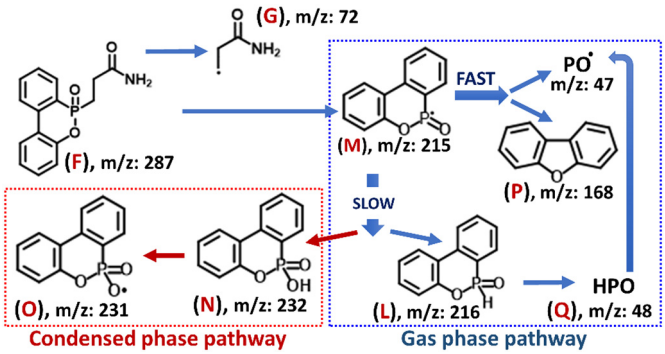

Scheme 1. Proposed pathways for gas phase and condensed phase mode of action of DA.

[25,41] and favoring flame inhibition. Accordingly, the gas phase mode of action is proposed for DA in Scheme 1.

Based on the discussion on degradation of epoxy resin, a general mode of reaction between DA and **EPO** during its degradation in air is proposed in Scheme S1. Oxygen may extract H• from the decomposition products of epoxy resin to form HO_2• and later transformed into OH• [22,41]. However, in the presence of DOPO radicals (species O and M of Scheme 1, Table S8), the active O• in the flame zone are neutralized and turned into a noticeable amount of volatile species such as PO•, PO_2• and $HOPO_2$• (flame inhibitors) [34]. This may strongly contribute to the flame retardancy of DA in the gas phase. Large amount of DOPO radicals (O and M species, Fig. S10) produced during the pyrolysis indicates a gas phase mechanism is involved for excellent performance in the UL test. DIP-MS analysis of **Mel** and **Si-Mel** showed the release of nitrogen species around 350 °C without any significant change in degradation of epoxy resin. Thus, the effect of melamine on the flame retardancy of silica-epoxy nanocomposites may be mainly ascribed to physical aspects. The nitrogen-based compound works as unreactive additive and diluent for the combustible gases, producing N_2 through its degradation [32–34]. Melamine has a physical role in the general mode of reaction between DA and **EPO**, influencing the flammability and ignition temperature of resin (Section 3.3, Table S6) without any chemical interaction with the main degradation products of epoxy. In view of the above, melamine does not appear in Scheme S1.

ATR-FTIR spectra of char after the vertical flame test of **EPO** and **Si-DA2-Mel** are shown in Figs. 7a and S12. Peaks at 661 cm^{-1} and 914 cm^{-1} corresponding to P—C and P–O–C stretching respectively in **Si-DA2-Mel** char indicates the presence of pyrophosphate and polyphosphates. The band at 1108 cm^{-1} can be attributed to stretching of silica units [16,42]. The C═C stretching vibration at 1589 cm^{-1} gives an evidence of carbonization [42,43] via dehydration of epoxy resin by acidic phosphorus species [22,25,44]. More detailed ATR-FTIR analysis is provided in Section S9. Higher P-content in **Si-DA2-Mel** char (4.1%) compared to unburnt **Si-DA2-Mel** (2.2%) was observed during EDX analysis (Fig. 7b). Moreover, Si/P ratio of 1.3 in char (Fig. 7b) is much higher than the sample prior to fire tests (0.5). ATR-FTIR and EDX analysis of **Si-DA2-Mel** char suggests that, in addition to the gas phase activity, DA acts also in the condensed phase.

3.5. Mechanical behavior

Tensile and flexural properties of **EPO**, **Si2** and **Si-DA2-Mel** samples were measured according to the ASTM D638 and ASTM D790 standards respectively (Fig. 7c, Tables S10 and S11). The presence of in-situ silica slightly increased the Young's modulus of **Si2** and reduced its fracture strength compared to **EPO**. The addition of melamine and DA reduced the fracture energy of the composites, resulting in an additional detrimental effect on fracture strength and toughness (Tables S10 and S11). On the contrary, ~34% increase in the Young's modulus can be due to the steric hindrance of the aromatic groups in DA, which decreases the motion of the molecular chains which leads to topological constrain [45]. This results in reduction in the plasticizing effect of DA on epoxy [26,45]. Presence of DA and melamine reduced the amount of energy required to fracture the material, inducing cracks fracture easily [46], even though significant improvement in flexural modulus (E_B) of **Si-DA2-Mel** was observed (Table S11).

4. Conclusions

In this work, an “in-situ” sol–gel synthesis was applied to an epoxy resin cured with a cycloaliphatic amine and the epoxy system was modified by adding DA and melamine. Presence of DA increased the thermo-oxidative stability of the epoxy system and the residues at high temperatures. Its addition to epoxy resin help achieve a strong reduction in the HRR (up to 70%) and increased the flashover time compared to the pristine epoxy resin. Inclusion of silica and melamine to the composite

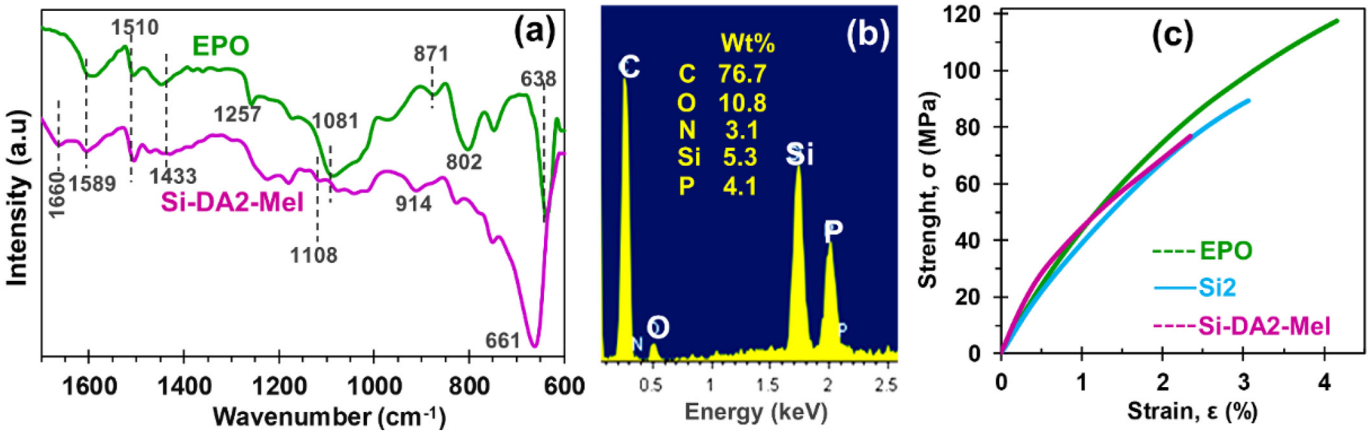

Fig. 7. (a) ATR-FTIR spectra of chars after the vertical burning test. (b) EDX spectrum of chars obtained after the vertical burning test of **Si-DA2-Mel**. (c) Tensile test results of **EPO**, **Si2** and **Si-DA2-Mel**.

system prevented melt dripping and increased the ignition time respectively. Combination of all these features achieved UL 94-V0 classification for epoxy resin composite at low P-content (2.0 wt%) and silica concentration (2.0 wt%). DIP-MS and PY-GC–MS analysis confirmed a main gas phase activity of DA for flame inhibition. ATR-FTIR and EDX analysis of the char confirmed that DA also plays a role in the condensed phase in presence of melamine and forms a phosphorus rich intumescent char. Presence of DA, silica nanoparticles and melamine resulted a reduction in the fracture strength and toughness, though a strong increase in the Young modulus was observed.

CRediT authorship contribution statement

Aurelio Bifulco: Investigation, Formal analysis. **Dambarudhar Parida:** Investigation, Formal analysis. **Khalifah A. Salmeia:** Formal analysis. **Rashid Nazir:** Investigation. **Sandro Lehner:** Investigation. **Rolf Stämpfli:** Investigation. **Hilber Markus:** Investigation. **Giulio Malucelli:** Project administration, Formal analysis, Investigation. **Francesco Branda:** Project administration, Formal analysis, Investigation. **Sabyasachi Gaan:** Project administration, Formal analysis, Investigation.

Declaration of competing interest

The authors declare no conflict of interest.

Acknowledgements

We are very thankful to Ms. Milijana Jovic (Advanced Fibers, Empa, St. Gallen, Switzerland) for her valuable support during the cone calorimeter and pyrolysis flow combustion calorimetry tests. The manuscript was written through contributions of all authors. All authors have given approval to the final version of the manuscript.

Appendix A. Supplementary data

Supplementary data to this article can be found online at https://doi.org/10.1016/j.matdes.2020.108862.

References

[1] J. Zhang, X. Mi, S. Chen, Z. Xu, D. Zhang, M. Miao, J. Wang, A bio-based hyperbranched flame retardant for epoxy resins, Chem. Eng. J. 381 (2020), 122719. .
[2] X. Zhao, D. Xiao, J.P. Alonso, D.-Y. Wang, Inclusion complex between beta-cyclodextrin and phenylphosphonicdiamide as novel bio-based flame retardant to epoxy: inclusion behavior, characterization and flammability, Mater. Des. 114 (2017) 623–632.
[3] Z. Qu, K. Wu, E. Jiao, W. Chen, Z. Hu, C. Xu, J. Shi, S. Wang, Z. Tan, Surface functionalization of few-layer black phosphorene and its flame retardancy in epoxy resin, Chem. Eng. J. 382 (2020), 122991. .
[4] H. Duan, Y. Chen, S. Ji, R. Hu, H. Ma, A novel phosphorus/nitrogen-containing polycarboxylic acid endowing epoxy resin with excellent flame retardance and mechanical properties, Chem. Eng. J. 375 (2019), 121916. .
[5] X.-F. Liu, B.-W. Liu, X. Luo, D.-M. Guo, H.-Y. Zhong, L. Chen, Y.-Z. Wang, A novel phosphorus-containing semi-aromatic polyester toward flame retardancy and enhanced mechanical properties of epoxy resin, Chem. Eng. J. 380 (2020), 122471. .
[6] L. Guadagno, M. Raimondo, V. Vittoria, L. Vertuccio, C. Naddeo, S. Russo, B. De Vivo, P. Lamberti, G. Spinelli, V. Tucci, Development of epoxy mixtures for application in aeronautics and aerospace, RSC Adv. 4 (2014) 15474–15488.
[7] L.B. Bourne, F.J. Milner, K.B. Alberman, Health problems of epoxy resins and amine-curing agents, Br. J. Ind. Med. 16 (1959) 81–97.
[8] J.S.P. Georlette, L. Costa, Halogen-containing Fire-retardant Compounds, Marcel Dekker, Inc, New York, 2000.
[9] P.M. Vikash, Y. Arao, Polymer Blends, Composites and Nanocomposites, Springer, Berlin, 2015.
[10] W. Wang, Y. Kan, B. Yu, Y. Pan, K.M. Liew, L. Song, Y. Hu, Synthesis of MnO2 nanoparticles with different morphologies and application for improving the fire safety of epoxy, Compos. Part A Appl. Sci. Manuf. 95 (2017) 173–182.
[11] W. Wang, Y. Kan, K. Meow Liew, L. Song, Y. Hu, Comparative investigation on combustion property and smoke toxicity of epoxy resin filled with α- and δ-MnO2 nanosheets, Compos. Part A Appl. Sci. Manuf. 107 (2018) 39–46.
[12] E. Bakhshandeh, A. Jannesari, Z. Ranjbar, S. Sobhani, M.R. Saeb, Anti-corrosion hybrid coatings based on epoxy–silica nano-composites: toward relationship between the morphology and EIS data, Prog. Org. Coat. 77 (2014) 1169–1183.
[13] L. Matějka, O. Dukh, J. Kolařík, Reinforcement of crosslinked rubbery epoxies by in-situ formed silica, Polymer 41 (2000) 1449–1459.
[14] J. Jiao, P. Liu, L. Wang, Y. Cai, One-step synthesis of improved silica/epoxy nanocomposites with inorganic-organic hybrid network, J. Polym. Res. 20 (2013) 202.
[15] Y. Zhu, B. Di, H. Chen, X. Wang, Y. Tian, In situ synthesis of novel biomass lignin/silica based epoxy resin adhesive from renewable resources at different pHs, J. Adhes. Sci. Technol. 33 (2019) 1806–1820.
[16] A. Bifulco, F. Tescione, A. Capasso, P. Mazzei, A. Piccolo, M. Durante, M. Lavorgna, G. Malucelli, F. Branda, Effects of post cure treatment in the glass transformation range on the structure and fire behavior of in situ generated silica/epoxy hybrids, J. Sol-Gel Sci. Technol. 87 (2018) 156–169.
[17] B.A. Howell, G.W. Lienhart, V.J. Livingstone, D. Aulakh, 1-Dopyl-1,2-(4-hydroxyphenyl)ethene: a flame retardant hardner for epoxy resin, Polym. Degrad. Stab. 175 (2020) 109110.
[18] M. Häublein, K. Peter, G. Bakis, R. Mäkimieni, V. Altstädt, M. Möller, Investigation on the flame retardant properties and fracture toughness of DOPO and nano-SiO (2) modified epoxy novolac resin and evaluation of its combinational effects, Materials 12 (2019).
[19] X. Qian, L. Song, Y. Bihe, B. Yu, Y. Shi, Y. Hu, R.K.K. Yuen, Organic/inorganic flame retardants containing phosphorus, nitrogen and silicon: preparation and their performance on the flame retardancy of epoxy resins as a novel intumescent flame retardant system, Mater. Chem. Phys. 143 (2014) 1243–1252.
[20] M. Rakotomalala, S. Wagner, M. Döring, Recent developments in halogen free flame retardants for epoxy resins for electrical and electronic applications, Materials 3 (2010) 4300–4327.
[21] S.L. Waaijers, J. Hartmann, A.M. Soeter, R. Helmus, S.A.E. Kools, P. de Voogt, W. Admiraal, J.R. Parsons, M.H.S. Kraak, Toxicity of new generation flame retardants to Daphnia magna, Sci. Total Environ. 463-464 (2013) 1042–1048.
[22] K.A. Salmeia, A. Gooneie, P. Simonetti, R. Nazir, J.-P. Kaiser, A. Rippl, C. Hirsch, S. Lehner, P. Rupper, R. Hufenus, S. Gaan, Comprehensive study on flame retardant polyesters from phosphorus additives, Polym. Degrad. Stab. 155 (2018) 22–34.

[23] R. Stämpfli, P.A. Brühwiler, I. Rechsteiner, V.R. Meyer, R.M. Rossi, X-ray tomographic investigation of water distribution in textiles under compression–possibilities for data presentation, Measurement 46 (2013) 1212–1219.
[24] F.G. Garcia, B.G. Soares, Determination of the epoxide equivalent weight of epoxy resins based on diglycidyl ether of bisphenol A (DGEBA) by proton nuclear magnetic resonance, Polym. Test. 22 (2003) 51–56.
[25] X. Liu, K.A. Salmeia, D. Rentsch, J. Hao, S. Gaan, Thermal decomposition and flammability of rigid PU foams containing some DOPO derivatives and other phosphorus compounds, J. Anal. Appl. Pyrolysis 124 (2017) 219–229.
[26] F. Wang, S. Pan, P. Zhang, H. Fan, Y. Chen, J. Yan, Synthesis and application of phosphorus-containing flame retardant plasticizer for polyvinyl chloride, Fibers and Polym 19 (2018) 1057–1063.
[27] N. Grassie, M.I. Guy, N.H. Tennent, Degradation of epoxy polymers: part 1—products of thermal degradation of bisphenol-A diglycidyl ether, Polym. Degrad. Stab. 12 (1985) 65–91.
[28] H. Yan, C.-x. Lu, D.-q. Jing, X.-l. Hou, Chemical degradation of amine-cured DGEBA epoxy resin in supercritical 1-propanol for recycling carbon fiber from composites, Chin. J. Polym. Sci. 32 (2014) 1550–1563.
[29] H. Yan, C. Lu, D. Jing, X. Hou, Chemical degradation of TGDDM/DDS epoxy resin in supercritical 1-propanol: promotion effect of hydrogenation on thermolysis, Polym. Degrad. Stab. 98 (2013) 2571–2582.
[30] P. Musto, Two-dimensional FTIR spectroscopy studies on the thermal-oxidative degradation of epoxy and epoxy−bis(maleimide) networks, Macromolecules 36 (2003) 3210–3221.
[31] G. Zhan, L. Zhang, Y. Tao, Y. Wang, X. Zhu, D. Li, Anodic ammonia oxidation to nitrogen gas catalyzed by mixed biofilms in bioelectrochemical systems, Electrochim. Acta 135 (2014) 345–350.
[32] K. Bretterbauer, C. Schwarzinger, Melamine derivatives - a review on synthesis and application, Curr. Org. Synth. 9 (2012) 342–356.
[33] S. Bourbigot, S. Duquesne, Fire retardant polymers: recent developments and opportunities, J. Mater. Chem. 17 (2007) 2283–2300.
[34] K.A. Salmeia, S. Gaan, An overview of some recent advances in DOPO-derivatives: chemistry and flame retardant applications, Polym. Degrad. Stab. 113 (2015) 119–134.
[35] J.W. Gilman, R.H. Harris Jr., J.R. Shields, T. Kashiwagi, A.B. Morgan, A study of the flammability reduction mechanism of polystyrene-layered silicate nanocomposite: layered silicate reinforced carbonaceous char, Polym. Adv. Technol. 17 (2006) 263–271.
[36] Q. Li, P. Jiang, Z. Su, P. Wei, G. Wang, X. Tang, Synergistic effect of phosphorus, nitrogen, and silicon on flame-retardant properties and char yield in polypropylene, J. Appl. Polym. Sci. 96 (2005) 854–860.
[37] H. Vahabi, B.K. Kandola, M.R. Saeb, Flame retardancy index for thermoplastic composites, Polymers 11 (2019) 407.
[38] H.V. Elnaz Movahedifar, Mohammad Reza Saeb, Sabu Thomas, Flame retardant epoxy composites on the road of innovation: an analysis with flame retardancy index for future development, Molecules 24 (2019) 47.
[39] R.E. Lyon, P.N. Balaguru, A. Foden, J. Davidovits, M. Davidovits, Fire response of geopolymer structural composites, The First International Conference on Composites in Infrastructure (ICCI' 96),Tuscon 1996, pp. 972–981.
[40] S. Molyneux, A.A. Stec, T.R. Hull, The effect of gas phase flame retardants on fire effluent toxicity, Polym. Degrad. Stab. 106 (2014) 36–46.
[41] A. Gooneie, P. Simonetti, K.A. Salmeia, S. Gaan, R. Hufenus, M.P. Heuberger, Enhanced PET processing with organophosphorus additive: flame retardant products with added-value for recycling, Polym. Degrad. Stab. 160 (2019) 218–228.
[42] R. Jian, P. Wang, W. Duan, J. Wang, X. Zheng, J. Weng, Synthesis of a novel P/N/S-containing flame retardant and its application in epoxy resin: thermal property, flame retardance, and pyrolysis behavior, Ind. Eng. Chem. Res. 55 (2016) 11520–11527.
[43] K.A. Salmeia, A. Neels, D. Parida, S. Lehner, D. Rentsch, S. Gaan, Insight into the synthesis and characterization of organophosphorus-based bridged triazine compounds, Molecules 24 (2019) 2672.
[44] R.R. Randle, D.H. Whiffen, The infra-red intensities of a band near 1020 cm^{-1} in mono- and para-substituted benzene derivatives, Trans. Faraday Soc. 52 (1956) 9–13.
[45] G. Luciani, A. Costantini, B. Silvestri, F. Tescione, F. Branda, A. Pezzella, Synthesis, structure and bioactivity of pHEMA/SiO2 hybrids derived through in situ sol–gel process, J. Sol-Gel Sci. Technol. 46 (2008) 166–175.
[46] H.C. Erythropel, S. Shipley, A. Börmann, J.A. Nicell, M. Maric, R.L. Leask, Designing green plasticizers: influence of molecule geometry and alkyl chain length on the plasticizing effectiveness of diester plasticizers in PVC blends, Polymer 89 (2016) 18–27.